Science Advances
AAAS

advances.sciencemag.org/cgi/content/full/7/3/eabd3207/DC1

Supplementary Materials for

O-GlcNAcylation ameliorates the pathological manifestations of Alzheimer's disease by inhibiting necroptosis

Jinsu Park, Hee-Jin Ha, Eun Seon Chung, Seung Hyun Baek, Yoonsuk Cho, Hark Kyun Kim, Jihoon Han, Jae Hoon Sul, Jeongmi Lee, Eunae Kim, Junsik Kim, Yong Ryoul Yang, Mikyoung Park, Sung Hyun Kim, Thiruma V. Arumugam, Hyemin Jang, Sang Won Seo, Pann-Ghill Suh, Dong-Gyu Jo*

*Corresponding author. Email: jodg@skku.edu

Published 13 January 2021, *Sci. Adv.* **7**, eabd3207 (2021)
DOI: 10.1126/sciadv.abd3207

This PDF file includes:

Supplementary Materials

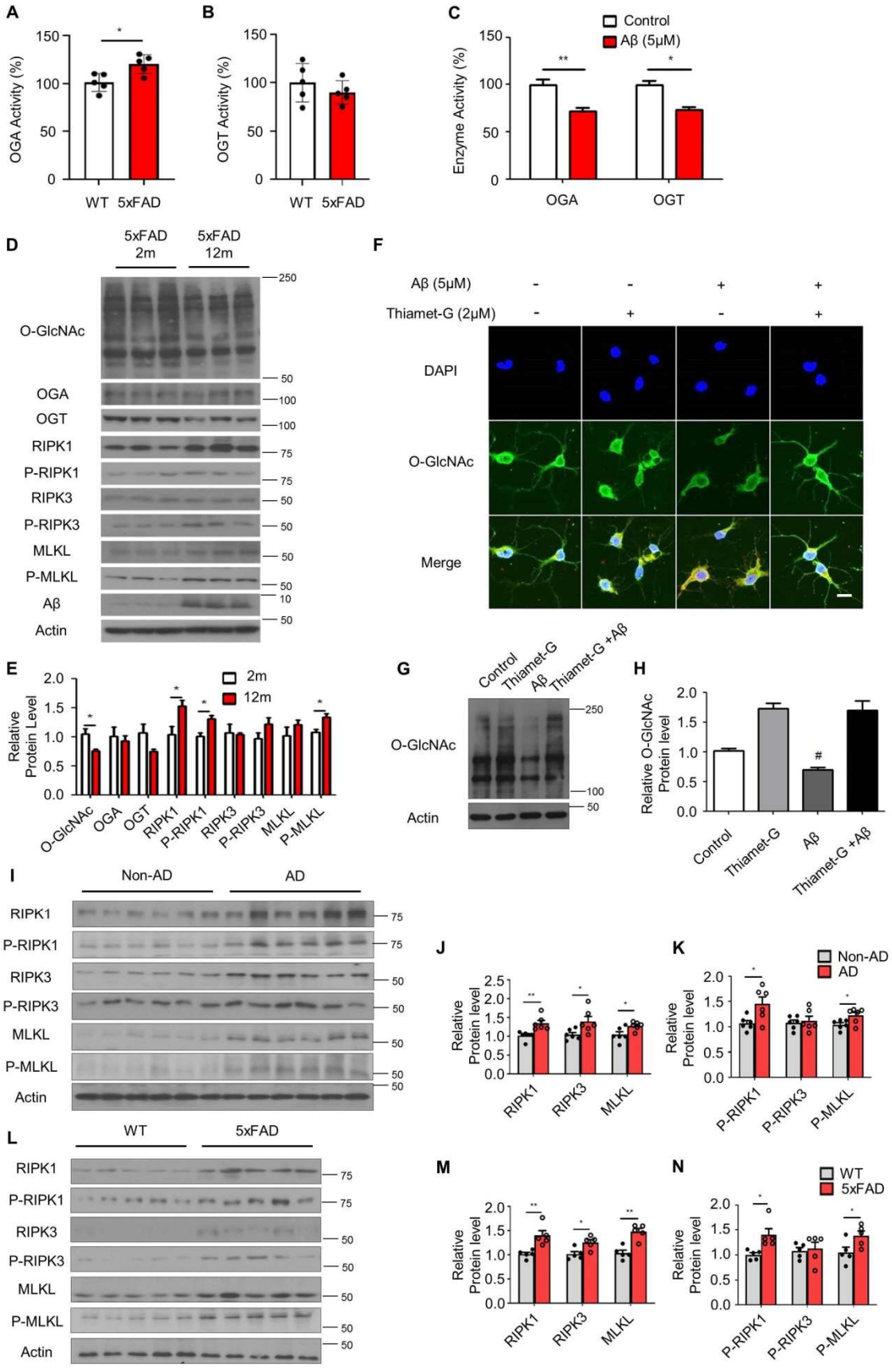

Fig. S1. O-GlcNAc levels are decreased and necroptosis factors were increased in the brain of AD patients and 5xFAD mice. (**A** and **B**) OGA (A) and OGT (B) activities in WT mice and 5xFAD mice (n = 5; 12 months of age). (C) OGA and OGT activities in rat primary neuron with exposure of Aβ (n = 4). (**D**) Western blot analysis of O-GlcNAcylation and necroptosis related proteins in brain tissues of 5xFAD at 2 and 12 months old (n = 3). (**E**) Quantification of proteins in fig. fig. S1D. (**F**) O-GlcNAc immunostaining in neurons with treating Aβ or thiamet-G; scale bar = 10 μm. (**G**) Western blot analysis of changes in the O-GlcNAcylation of cellular proteins by Aβ and thiamet-G. (**H**) Quantification of O-GlcNAc proteins in fig. S1G (n = 3). (**I**) Western blot analysis of necroptosis proteins in insoluble pellet in brain tissues of AD patients (n = 6) and controls without symptoms of dementia (non-AD; n = 6) (**J** and **K**) Quantification of necroptosis proteins (J) and phosphorylated necroptosis proteins (K) in fig. S1I. (**L**) Western blot analysis of necroptosis proteins in insoluble fractions of brain tissues of 5xFAD and WT mice (n = 5) (**M** and **N**) Quantification of necroptosis proteins (M) and phosphorylated necroptosis proteins (N) in fig. S1L. The levels of phosphorylated necroptosis-related proteins were normalized to the levels of the corresponding total proteins. Values are presented as means ± SEM. *P < 0.05 and **P < 0.01 versus non-AD (J and K) or WT (A, B, M and N) or 5xFAD 2m (E) or control (C); #P < 0.05 versus control (H); two-tailed Student's t test.

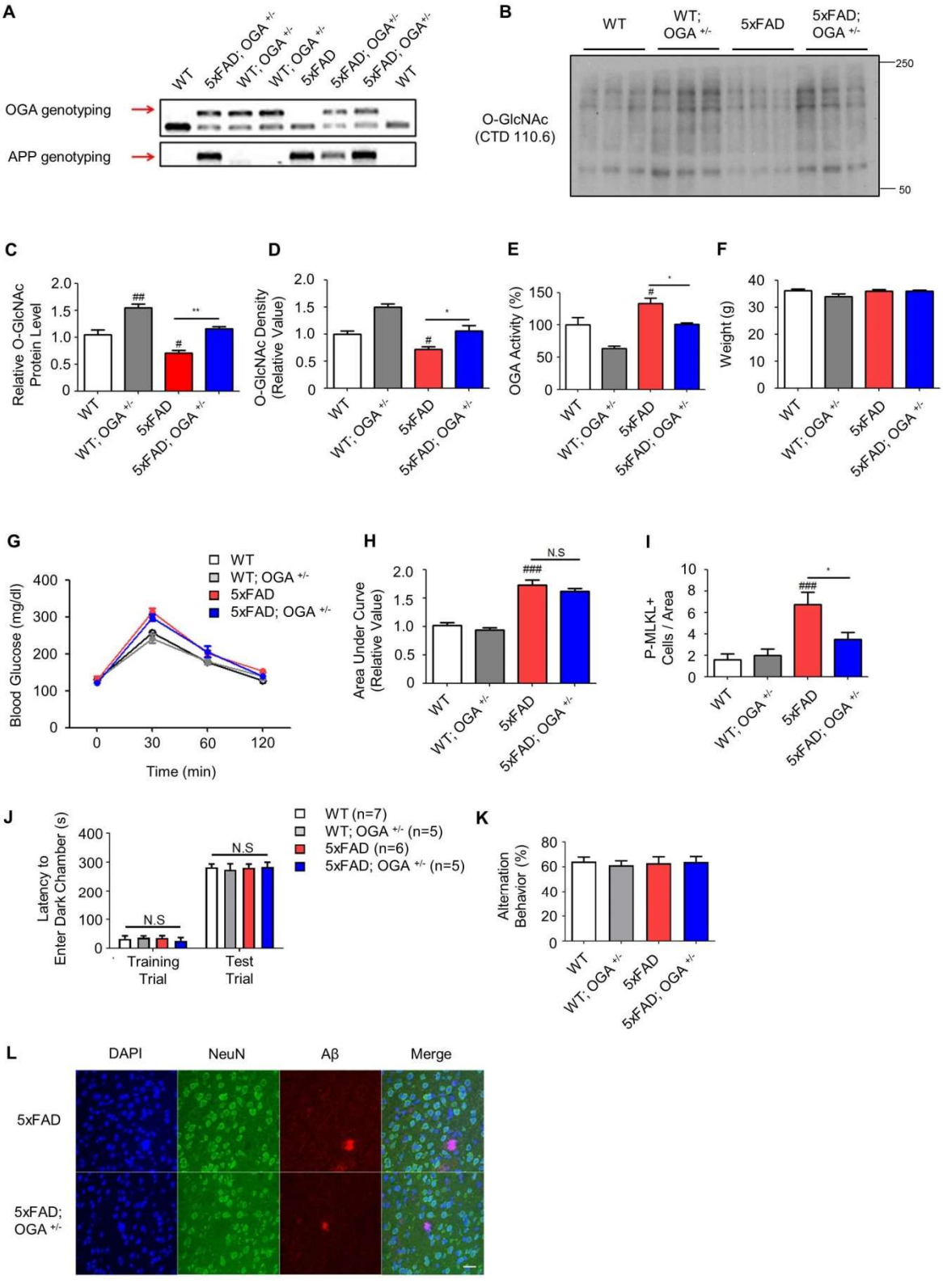
A
WT
5xFAD; OGA +/-
WT; OGA +/-
WT; OGA +/-
5xFAD
5xFAD; OGA +/-
5xFAD; OGA +/-
WT
OGA genotyping
APP genotyping
B
WT
WT; OGA +/-
5xFAD
5xFAD; OGA +/-
O-GlcNAc (CTD 110.6)
250
50
C
Relative O-GlcNAc Protein Level
D
O-GlcNAc Density (Relative Value)
E
OGA Activity (%)
F
Weight (g)
G
WT
WT; OGA +/-
5xFAD
5xFAD; OGA +/-
Blood Glucose (mg/dl)
Time (min)
H
Area Under Curve (Relative Value)
N.S
I
P-MLKL+ Cells / Area
J
WT (n=7)
WT; OGA +/- (n=5)
5xFAD (n=6)
5xFAD; OGA +/- (n=5)
Latency to Enter Dark Chamber (s)
Training Trial
Test Trial
K
Alternation Behavior (%)
L
DAPI
NeuN
Aβ
Merge
5xFAD
5xFAD; OGA +/-

Fig. S2. Experimental animals at 3 months did not show any AD symptoms. (**A**) Representative result of genotyping of the four types of mice; WT, WT;OGA$^{+/-}$, 5xFAD, and 5xFAD;OGA$^{+/-}$. (**B**) Western blot analysis of O-GlcNAcylated proteins using CTD 110.6 antibody in brain samples of indicated mouse genotypes (n = 3). (C) Quantification of O-GlcNAc protein level in fig. S2B. (**D**) Quantification of O-GlcNAc area in Fig. 2D. (**E**) Quantification of OGA activity in indicated genotypes of mice (n = 3 to 4 per groups). (**F**) The weight of indicated mouse genotypes used in behavioral tests. (**G**) Blood glucose during oral glucose tolerance test of indicated mouse genotypes at 16 weeks of age (n = 4). (**H**) Area under curve of fig. S2G. (**I**) The number of P-MLKL positive cells in Fig. 2D. (**J**) Time of memory retention in the passive avoidance test of indicated mouse genotypes; WT, WT;OGA$^{+/-}$, 5xFAD, and 5xFAD;OGA$^{+/-}$ at 3 months (n = 5 to 7). (**K**) The spontaneous alteration in Y-maze of indicated mouse genotypes at 3 months. (**L**) Immunostaining of NeuN and Aβ in the brain tissues of 5xFAD and 5xFAD; OGA $^{+/-}$ mice at 3 months; scale bar = 20 μm. Three slices of each sample were used to normalize each sample. Values are presented as means ± SEM. #P < 0.05, and ###P < 0.001 versus WT; *P < 0.05 versus 5xFAD; one-way ANOVA with Tukey's test. N.S: nonsignificant .

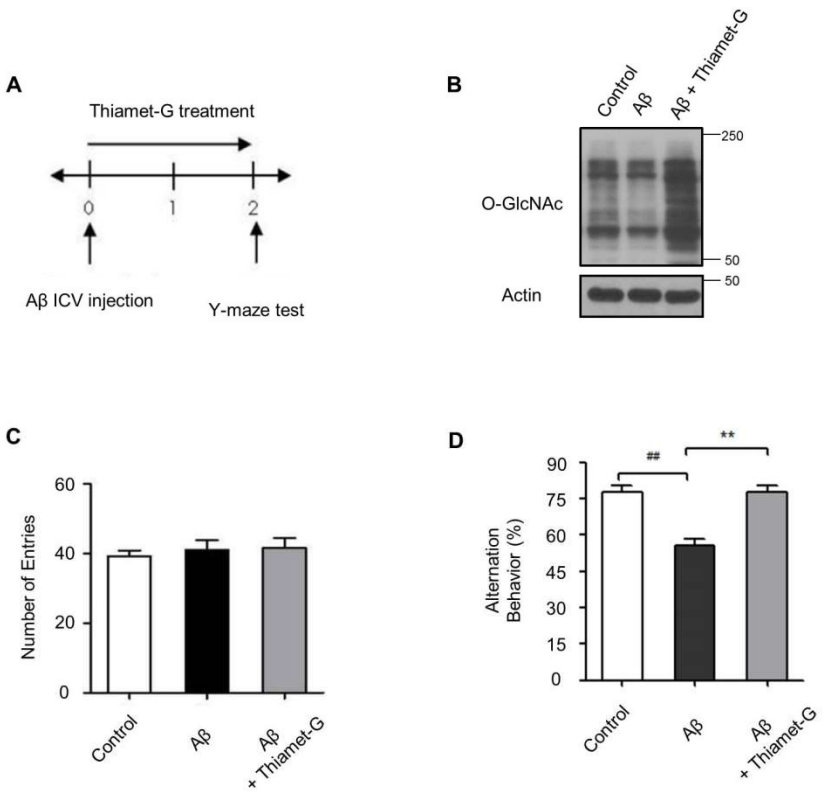

Fig. S3. OGA inhibitor rescued cognitive function in the Aβ-injected mice. (**A**) A schematic diagram of Aβ, drug treatment, and cognitive testing. (**B**) Western blot analysis of O-GlcNAc in brain samples of experimental mice (n = 3). (**C**) Analysis of the number of arm entries of experimental mice in the Y maze test (n = 6). (D) The evaluation of spontaneous alternation levels of each group in the Y maze test. Values are presented as means ± SEM. ##P < 0.01 versus Control; **P < 0.01 versus Aβ injected group; one-way ANOVA with Tukey's test.

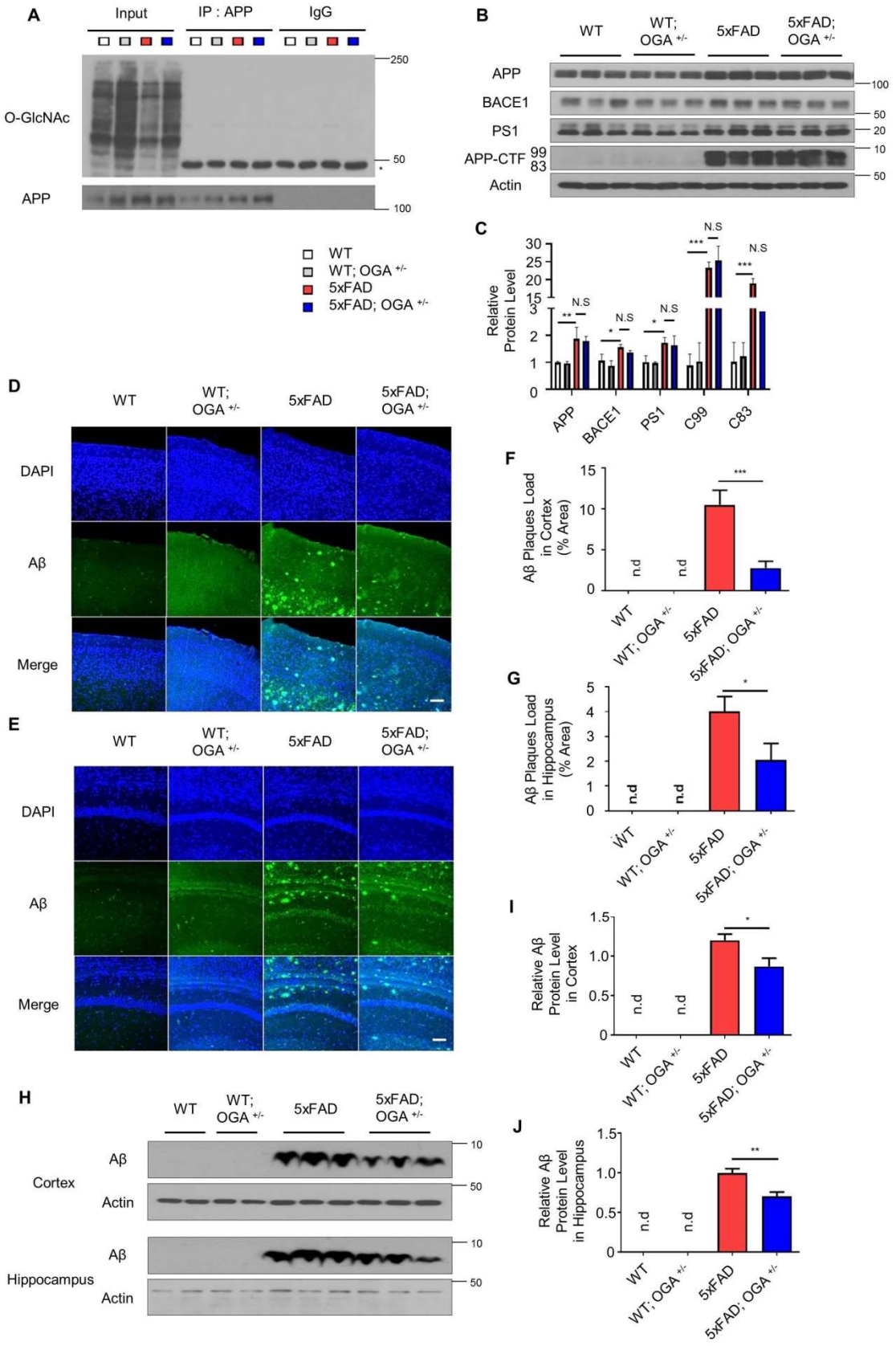
A
Input
IP : APP
IgG
O-GlcNAc
APP
250
50
100
WT
WT; OGA +/-
5xFAD
5xFAD; OGA +/-
B
WT
WT; OGA +/-
5xFAD
5xFAD; OGA +/-
APP
BACE1
PS1
APP-CTF
99
83
Actin
100
50
20
10
50
C
Relative Protein Level
N.S
APP
BACE1
PS1
C99
C83
D
WT
WT; OGA +/-
5xFAD
5xFAD; OGA +/-
DAPI
Aβ
Merge
E
WT
WT; OGA +/-
5xFAD
5xFAD; OGA +/-
DAPI
Aβ
Merge
F
Aβ Plaques Load in Cortex (% Area)
n.d
WT
WT; OGA +/-
5xFAD
5xFAD; OGA +/-
G
Aβ Plaques Load in Hippocampus (% Area)
n.d
WT
WT; OGA +/-
5xFAD
5xFAD; OGA +/-
H
WT
WT; OGA +/-
5xFAD
5xFAD; OGA +/-
Cortex
Aβ
Actin
Hippocampus
Aβ
Actin
10
50
10
50
I
Relative Aβ Protein Level in Cortex
n.d
WT
WT; OGA +/-
5xFAD
5xFAD; OGA +/-
J
Relative Aβ Protein Level in Hippocampus
n.d
WT
WT; OGA +/-
5xFAD
5xFAD; OGA +/-

Fig. S4. OGA haploinsufficiency did not affect the levels of proteins involved in amyloidogenesis in the brain tissue of 5xFAD mice, but decreased the Aβ burden in the brain tissue of 5xFAD mice. (**A**) Western blot analysis of O-GlcNAc proteins in APP immunoprecipitates from mice brain samples. The precipitated IgG heavy chain is marked with an asterisk. (B) Western blot analysis of expression of proteins related to APP processing in brain samples of indicated mouse genotypes (n = 3; 9 months of age). (**C**) Quantification of the expression of proteins related to APP processing in brain samples of 5xFAD mice and 5xFAD;OGA $^{+/-}$. (**D** and **E**) Aβ plaques in cortex (D) and hippocampus (E) of mice samples; scale bar = 100μm. (**F** and **G**) Quantification of Aβ plaques loads in cortex (F) and hippocampus (G) (n = 3 to 5). (**H**) Western blot analysis of Aβ expression in the cortex and hippocampus of indicated mouse genotypes (n = 3). (**I** and **J**) Quantification of Aβ expression in the cortex (I) and hippocampus (J) of indicated mouse genotypes. Three slices of each sample were used to normalize each sample. Values are presented as means ± SEM. *P < 0.05, **P < 0.01, ***P < 0.001 versus 5xFAD; one-way ANOVA with Tukey's test. N.S., nonsignificant; n.d., not detectable.

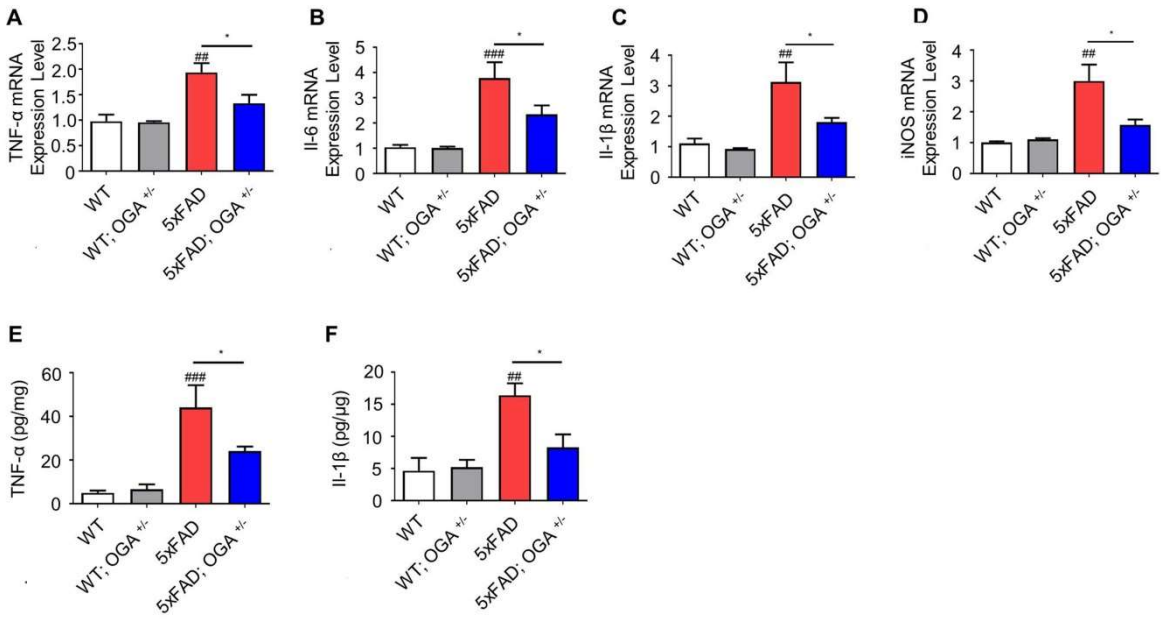

Fig. S5. Increasing O-GlcNAcylation alleviates neuroinflammatory responses. (**A** to **D**) mRNA levels of TNF-α (A), Il-6 (B), Il-1β (C), and iNOS (D) in mice brain samples (n = 4 to 6). (**E** and **F**) The levels of TNF-α (E) and IL-1β (F) proteins measured in mice brain samples (n = 3 to 5). Three slices of each sample were used to normalize each sample. Values are presented as means ± SEM. #P < 0.05, ##P < 0.01, and ###P < 0.001 versus WT; *P < 0.05 and **P < 0.01 versus 5xFAD (A to F); one-way ANOVA with Tukey's test.

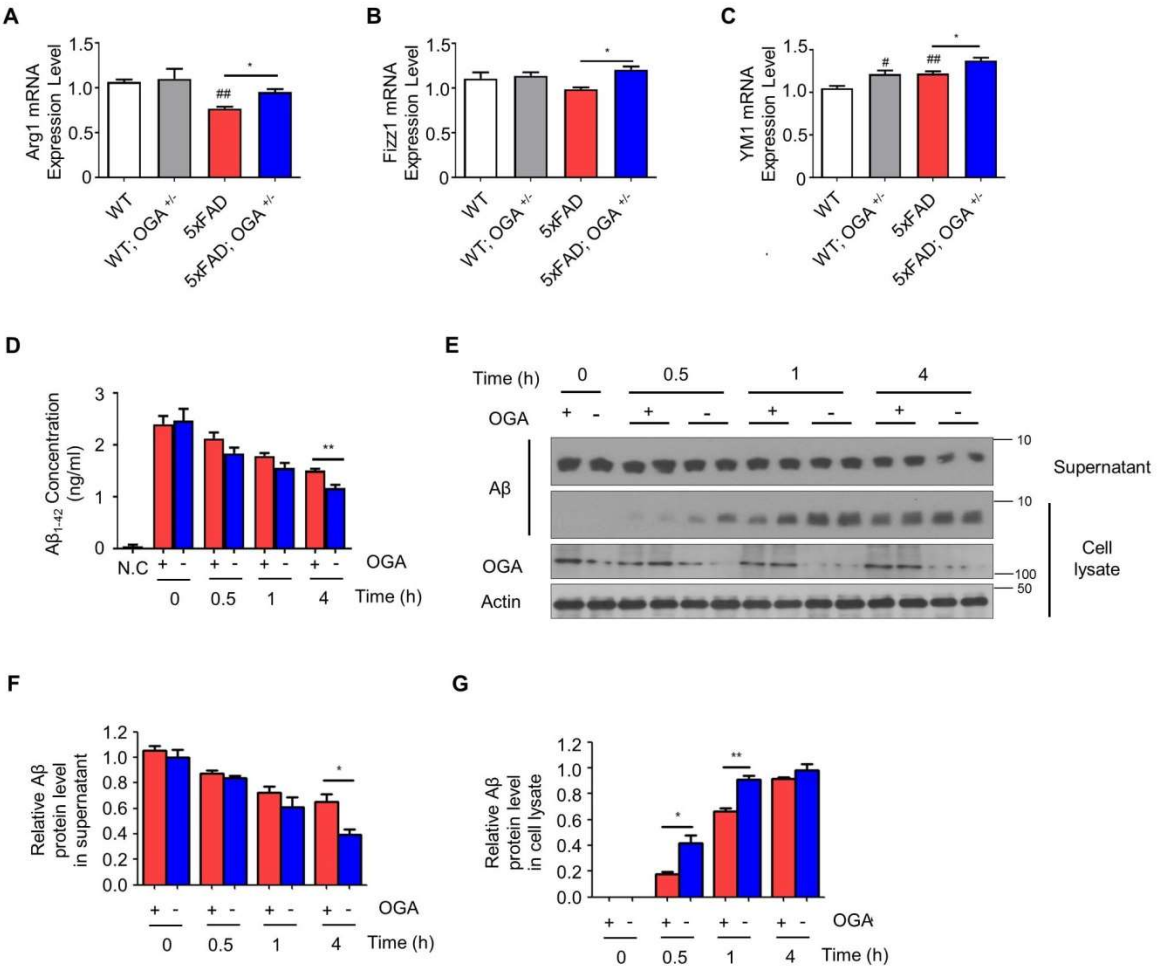

Fig. S6. Increasing O-GlcNAcylation alters polarization of microglia and increases phagocytic activity. (**A** to **C**) Levels of Arg 1 (A), Fizz1 (B), and YM1 (C) mRNA in mice brain samples (n = 3 to 5). (**D**) Levels of $A\beta_{42}$ remaining in the culture media with primary microglia measured by ELISA (n = 3). (**E**) Western blot analysis of extracellular and intracellular levels of $A\beta_{42}$ in primary microglia at each time point. (**F** and **G**) Quantification of Aβ proteins in supernatant (F) or cell lysate (G) in fig. S6E. Values are presented as means ± SEM. #P < 0.05, ##P < 0.01, and ###P < 0.001 versus WT; *P < 0.05 and **P < 0.01 versus 5xFAD (A to C) or WT microglia (D to G); one-way ANOVA with Tukey's test (A to C), two-tailed Student's t test (D to G).

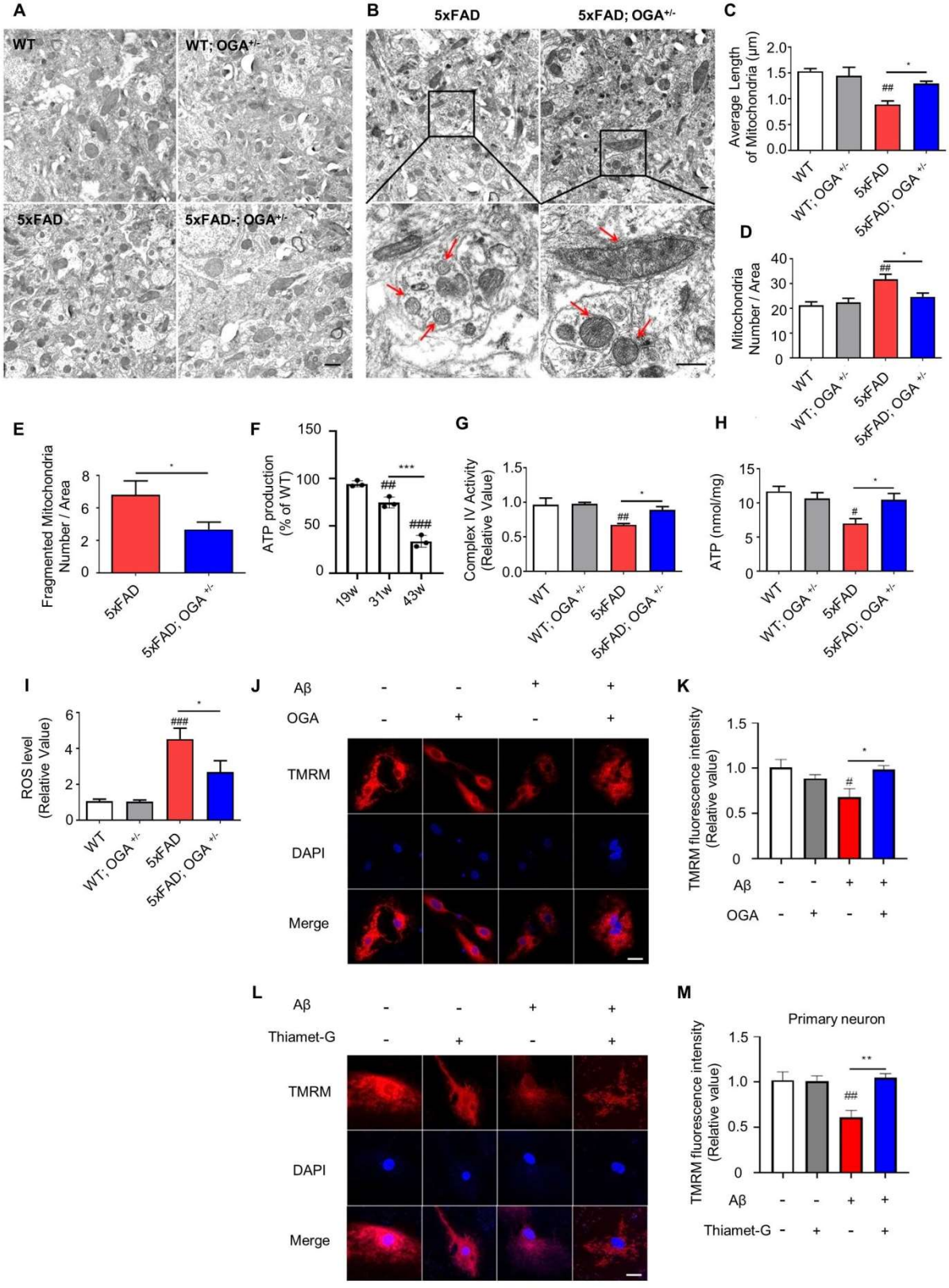
A
WT
WT; OGA+/-
5xFAD
5xFAD-; OGA+/-
B
5xFAD
5xFAD; OGA+/-
C
Average Length of Mitochondria (μm)
WT
WT; OGA +/-
5xFAD
5xFAD; OGA +/-
D
Mitochondria Number / Area
E
Fragmented Mitochondria Number / Area
F
ATP production (% of WT)
19w
31w
43w
G
Complex IV Activity (Relative Value)
H
ATP (nmol/mg)
I
ROS level (Relative Value)
J
Aβ
OGA
TMRM
DAPI
Merge
K
TMRM fluorescence intensity (Relative value)
L
Thiamet-G
M
Primary neuron

Fig. S7. O-GlcNAcylation rejuvenates damaged mitochondria. (**A**) TEM images of cortical region of mice samples (n = 4 to 7); scale bar = 1 μm. (**B**) TEM images at higher magnification of 5xFAD and 5xFAD; $OGA^{+/-}$ mice (n = 3 to 4); scale bar = 250 nm. (**C**) Quantification of average length of mitochondria in fig. S7A. (**D**) The number of mitochondria in fig. S7A. (**E**) The number of fragmented mitochondria in fig. S7B. (**F**) ATP production in the brain tissue of 5xFAD mice (n = 3). (**G**) Quantification of Complex IV activity in the brain of mice samples (n = 3 to 5). (**H**) ATP production in mitochondria of mice samples (n = 3 to 5; 9 months of age). (**I**) ROS levels in mitochondria of mice samples (n = 3 to 5). (**J**) Images of TMRM staining in primary neurons of WT or WT;$OGA^{+/-}$ mice exposed to Aβ (n = 3); scale bar = 20 μm. (**K**) Quantification of TMRM fluorescence intensity in fig. S7J. (**L**) Images of TMRM staining in rat primary neurons exposed to Aβ or treated with thiamet-G (n = 3); scale bar = 10 μm. (**M**) Quantification of TMRM fluorescence intensity in fig. S7L. Values are presented as means ± SEM. #P < 0.05, ##P < 0.01, and ###P < 0.001 versus WT (C to I) except for 19w (F) or control group (K and M); *P < 0.05, *P < 0.01, and ***P < 0.001 versus 5xFAD (C to I) except for 31 w (F) or Aβ exposed group (K and M); one-way ANOVA with Tukey's test except for two-tailed Student's t test (E).

Table S1. Clinical data of AD patients and non-demented control subjects

Patients	Age (years)	Gender	PMI (h)	Neuritic Plaques	Cause of death	Braak stage
AD patients						
1	83	Male	4.00	24.6	Aspiration pneumonia	6
2	78	Male	3.75	34.2	Unknown	6
3	84	Male	4.5	34.8	Unknown	6
4	86	Female	3.25	19.4	Respiratory infection	6
5	74	Male	3.00	27.2	Fall	6
6	90	Female	2.6	30.4	Unknown	6
Mean±S.D	82.5±5.22		3.51±0.63	28.43±5.40		
Non-demented						
1	81	Male	2.0	13.4	Pulmonary embolism	2
2	76	Female	2.0	0	Chronic obstructive pulmonary disease	1
3	85	Male	2.0	5.6	Unknown	3
4	74	Male	4.0	0	Congestive heart failure	1
5	86	Female	2.25	7.6	Unknown	2
6	86	Female	3.75	7.8	Cardiovascular disease	1
Mean±S.D	81.33±4.82		2.67±0.86	5.73±4.70		

Table S2. Antibody information

Name	Company	Cat. Number	Host	Reactivity	Molecular weight	Antibody concentration	
						W.B	Staining
Aβ	Abcam	Ab39377	R	H, M			1:1000
Aβ (6e10)	Biolegend	803004	M	H	10~	1: 1000	
APP	Biolegend	802801	M	H, M, R	100~150	1: 1000	
APP-CTF	Biolegend	802801	M	H, M, R	100~150(Full) 10~20(CTF)	1: 1000	
BACE1	Cell Signaling	5606	R	H, M, R	70	1:1000	
GFAP	Millipore	MAB360	M	H, M, R	51	1: 1000	1:500
Iba-1	Genetex	GTX632426	M	H, M, R	17	1: 1000	
Iba-1	Wako	019-19741	R	H, M, R			1:1000
MLKL	Millipore	CS214789	R	H	50~60	1: 1000	
MLKL	Millipore	MABC604	Rat	M	52	1: 1000	
NeuN	Millipore	MAB377	M	H, M, R			1:1000
NeuN-488	Abcam	Ab190194	R	H, M, R			1:100
OGA	Novus	NBP1-81244	R	H, M, R	130	1: 1000	
O-Glcnac	Invitrogen	MA1-072	M	H, M, R	40~	1: 1000	1:250
O-GlcNAc	Cell Signaling	9875	M	All	40~	1: 1000	
OGT	Abcam	Ab96718	R	H, M, R	117	1: 2000	
P-MLKL	Abcam	Ab196436	R	M	54	1: 1000	1:100
P-MLKL	Millipore	CS214775	R	H	50~60	1: 1000	

P-RIPK1	Cell Signaling	31122s	R	M	80	1: 1000	
P-RIPK1	Cell Signaling	65746	R	H	80	1: 1000	
P-RIPK3	Cell Signaling	57220	R	M	55	1: 1000	
P-RIPK3	Cell Signaling	93654	R	H	55	1: 1000	
PS1	Cell Signaling	5643	R	H, M, R	20~25	1: 1000	
RIPK1	BD Sciences	610458	M	H, M, R	74	1: 1000	
RIPK3	Abcam	Ab56164	R	H, M	54	1: 500	
Synaptophysin	Abcam	Ab8049	M	H, M, R	38	1:500	1:100

Table S3. qRT-PCR primer information

Primer name	**Sequence (Forward)**	**Sequence (Reverse)**	**Reference**
TNF-α	CAGAGGGCCTGTACCTCATCc	GGAAGACCCCTCCCAGATAG	(40)
Il-6	AATTCGGTACATCCTCGACGG	TTGGAAGGTTCAGGTTGTTTTC	(40)
Il-1β	AGCTGGATGCTCTCATCAGG	AGTTGACGGACCCCAAAAG	
iNOS	GGGCTGTCACGGAGATCA	CCATGATGGTCACATTCTGC	
Arg1	TCACCTGAGCTTTGATGTCG	CTGAAAGGAGCCCTGTCTTG	(*51*)
Fizz1	CTGATGAGACCATAGAGATTATCGTG	GCACAGGCAGTTGCAAGTATCTCC	(*52*)
YM1	CGAGGTAATGAGTGGGTTGG	CACGGCACCTCCTAAATTGT	(*51*)
GAPDH	TGTCCGTCGTGGATCTGAC	CGTGCTTCACCACCTTCTTG	

REFERENCES AND NOTES

1. J. Wang, B. J. Gu, C. L. Masters, Y.-J. Wang, A systemic view of Alzheimer disease—Insights from amyloid-β metabolism beyond the brain. *Nat. Rev. Neurol.* **13**, 612–623 (2017).

2. H. Lee, D. Kim, W. Lee, H. Y. Kim, Y. Kim, Preventive approach for overcoming dementia. *Arch. Pharm. Res.* **42**, 647–657 (2019).

3. G. Livingston, A. Sommerlad, V. Orgeta, S. G. Costafreda, J. Huntley, D. Ames, C. Ballard, S. Banerjee, A. Burns, J. Cohen-Mansfield, C. Cooper, N. Fox, L. N. Gitlin, R. Howard, H. C. Kales, E. B. Larson, K. Ritchie, K. Rockwood, E. L. Sampson, Q. Samus, L. S. Schneider, G. Selbæk, L. Teri, N. Mukadam, Dementia prevention, intervention, and care. *Lancet* **390**, 2673–2734 (2017).

4. Q. Li, B. A. Barres, Microglia and macrophages in brain homeostasis and disease. *Nat. Rev. Immunol.* **18**, 225–242 (2018).

5. A. Caccamo, C. Branca, I. S. Piras, E. Ferreira, M. J. Huentelman, W. S. Liang, B. Readhead, J. T. Dudley, E. E. Spangenberg, K. N. Green, R. Belfiore, W. Winslow, S. Oddo, Necroptosis activation in Alzheimer's disease. *Nat. Neurosci.* **20**, 1236–1246 (2017).

6. L. Galluzzi, G. Kroemer, Necroptosis: A specialized pathway of programmed necrosis. *Cell* **135**, 1161–1163 (2008).

7. D. C. Rubinsztein, RIPK1 promotes inflammation and β-amyloid accumulation in Alzheimer's disease. *Proc. Natl. Acad. Sci. U.S.A.* **114**, 10813–10814 (2017).

8. J. Yuan, P. Amin, D. Ofengeim, Necroptosis and RIPK1-mediated neuroinflammation in CNS diseases. *Nat. Rev. Neurosci.* **20**, 19–33 (2019).

9. S.-H. Yang, D. K. Lee, J. Shin, S. Lee, S. Baek, J. Kim, H. Jung, J.-M. Hah, Y. Kim, Nec-1 alleviates cognitive impairment with reduction of Aβ and tau abnormalities in APP/PS1 mice. *EMBO Mol. Med.* **9**, 61–77 (2016).

10. Y. Ito, D. Ofengeim, A. Najafov, S. Das, S. Saberi, Y. Li, J. Hitomi, H. Zhu, H. Chen, L. Mayo, J. Geng, P. Amin, J. P. DeWitt, A. K. Mookhtiar, M. Florez, A. T. Ouchida, J.-b. Fan, M. Pasparakis, M.

A. Kelliher, J. Ravits, J. Yuan, RIPK1 mediates axonal degeneration by promoting inflammation and necroptosis in ALS. *Science* **353**, 603–608 (2016).

11. D. Ofengeim, Y. Ito, A. Najafov, Y. Zhang, B. Shan, J. P. DeWitt, J. Ye, X. Zhang, A. Chang, H. Vakifahmetoglu-Norberg, J. Geng, B. Py, W. Zhou, P. Amin, J. Berlink Lima, C. Qi, Q. Yu, B. Trapp, J. Yuan, Activation of necroptosis in multiple sclerosis. *Cell Rep.* **10**, 1836–1849 (2015).

12. A. Iannielli, S. Bido, L. Folladori, A. Segnali, C. Cancellieri, A. Maresca, L. Massimino, A. Rubio, G. Morabito, L. Caporali, F. Tagliavini, O. Musumeci, G. Gregato, E. Bezard, V. Carelli, V. Tiranti, V. Broccoli, Pharmacological inhibition of necroptosis protects from dopaminergic neuronal cell death in Parkinson's disease models. *Cell Rep.* **22**, 2066–2079 (2018).

13. J. Park, M. K. P. Lai, T. V. Arumugam, D.-G. Jo, O-GlcNAcylation as a therapeutic target for Alzheimer's disease. *Neuromol. Med.* **22**, 171–193 (2020).

14. Y. E. Lewis, A. Galesic, P. M. Levine, C. A. De Leon, N. Lamiri, C. K. Brennan, M. R. Pratt, O-GlcNAcylation of α-synuclein at serine 87 reduces aggregation without affecting membrane binding. *ACS Chem. Biol.* **12**, 1020–1027 (2017).

15. N. B. Hastings, X. Wang, L. Song, B. D. Butts, D. Grotz, R. Hargreaves, J. F. Hess, K.-L. K. Hong, C. R.-R. Huang, L. Hyde, M. Laverty, J. Lee, D. Levitan, S. X. Lu, M. Maguire, V. Mahadomrongkul, E. J. McEachern, X. Ouyang, T. W. Rosahl, H. Selnick, M. Stanton, G. Terracina, D. J. Vocadlo, G. Wang, J. L. Duffy, E. M. Parker, L. Zhang, Inhibition of O-GlcNAcase leads to elevation of O-GlcNAc tau and reduction of taupathy and cerebrospinal fluid tau in rTg4510 mice. *Mol. Neurodegener.* **12**, 39 (2017).

16. S. A. Yuzwa, X. Shan, M. S. Macauley, T. Clark, Y. Skorobogatko, K. Vosseller, D. J. Vocadlo, Increasing *O*-GlcNAc slows neurodegeneration and stabilizes tau against aggregation. *Nat. Chem. Biol.* **8**, 393–399 (2012).

17. Y. Gao, L. Wells, F. I. Comer, G. J. Parker, G. W. Hart, Dynamic O–glycosylation of nuclear and cytosolic proteins: Cloning and characterization of a neutral, cytosolic beta-N-acetylglucosaminidase from human brain. *J. Biol. Chem.* **276**, 9838–9845 (2001).

18. Y. R. Yang, M. Song, H. Lee, Y. Jeon, E.-J. Choi, H.-J. Jang, H. Y. Moon, H.-Y. Byun, E.-K. Kim, D. H. Kim, M. N. Lee, A. Koh, J. Ghim, J. H. Choi, W. Lee-Kwon, K. T. Kim, S. H. Ryu, P.-G. Suh, O-GlcNAcase is essential for embryonic development and maintenance of genomic stability. *Aging Cell* **11**, 439–448 (2012).

19. T. S. Pinho, S. C. Correia, G. Perry, A. F. Ambrósio, P. I. Moreira, Diminished O-GlcNAcylation in Alzheimer's disease is strongly correlated with mitochondrial anomalies. *Biochim. Biophys. Acta Mol. Basis Dis.* **1865**, 2048–2059 (2019).

20. F. Liu, J. Shi, H. Tanimukai, J. Gu, J. Gu, I. Grundke-Iqbal, K. Iqbal, C.-X. Gong, Reduced O-GlcNAcylation links lower brain glucose metabolism and tau pathology in Alzheimer's disease. *Brain* **132**, 1820–1832 (2009).

21. A. C. Wang, E. H. Jensen, J. E. Rexach, H. V. Vinters, L. C. Hsieh-Wilson, Loss of *O*-GlcNAc glycosylation in forebrain excitatory neurons induces neurodegeneration. *Proc. Natl. Acad. Sci. U.S.A.* **113**, 15120–15125 (2016).

22. S. A. Yuzwa, X. Shan, B. A. Jones, G. Zhao, M. L. Woodward, X. Li, Y. Zhu, E. J. McEachern, M. A. Silverman, N. V. Watson, C.-X. Gong, D. J. Vocadlo, Pharmacological inhibition of *O*-GlcNAcase (OGA) prevents cognitive decline and amyloid plaque formation in bigenic tau/APP mutant mice. *Mol. Neurodegener.* **9**, 42 (2014).

23. E. P. Tan, S. R. McGreal, S. Graw, R. Tessman, S. J. Koppel, P. Dhakal, Z. Zhang, M. Machacek, N. E. Zachara, D. C. Koestler, K. R. Peterson, J. P. Thyfault, R. H. Swerdlow, P. Krishnamurthy, L. DiTacchio, U. Apte, C. Slawson, Sustained *O*-GlcNAcylation reprograms mitochondrial function to regulate energy metabolism. *J. Biol. Chem.* **292**, 14940–14962 (2017).

24. M.-Y. Cha, H. J. Cho, C. Kim, Y. O. Jung, M. J. Kang, M. E. Murray, H. S. Hong, Y.-J. Choi, H. Choi, D. K. Kim, H. Choi, J. Kim, D. W. Dickson, H. K. Song, J. W. Cho, E. C. Yi, J. Kim, S. M. Jin, I. Mook-Jung, Mitochondrial ATP synthase activity is impaired by suppressed *O*-GlcNAcylation in Alzheimer's disease. *Hum. Mol. Genet.* **24**, 6492–6504 (2015).

25. J. Li, T. McQuade, A. B. Siemer, J. Napetschnig, K. Moriwaki, Y.-S. Hsiao, E. Damko, D. Moquin, T. Walz, A. McDermott, F. K.-M. Chan, H. Wu, The RIP1/RIP3 necrosome forms a functional amyloid signaling complex required for programmed necrosis. *Cell* **150**, 339–350 (2012).

26. M. S. Macauley, X. Shan, S. A. Yuzwa, T. M. Gloster, D. J. Vocadlo. Elevation of global *O*-GlcNAc in rodents using a selective *O*-GlcNAcase inhibitor does not cause insulin resistance or perturb glucohomeostasis. *Chem. Biol.* **17**, 949–958 (2010).

27. C. Keembiyehetty, D. C. Love, K. R. Harwood, O. Gavrilova, M. E. Comly, J. A. Hanover. Conditional knock-out reveals a requirement for *O*-linked N-acetylglucosaminase (*O*-GlcNAcase) in metabolic homeostasis. *J. Biol. Chem.* **290**, 7097–7113 (2015).

28. H. Oakley, S. L. Cole, S. Logan, E. Maus, P. Shao, J. Craft, A. Guillozet-Bongaarts, M. Ohno, J. Disterhoft, L. V. Eldik, R. Berry, R. Vassar. Intraneuronal β-amyloid aggregates, neurodegeneration, and neuron loss in transgenic mice with five familial Alzheimer's disease mutations: Potential factors in amyloid plaque formation. *J. Neurosci.* **26**, 10129–10140 (2006).

29. O. Butovsky, H. L. Weiner, Microglial signatures and their role in health and disease. *Nat. Rev. Neurosci.* **19**, 622–635 (2018).

30. S. H. Baek, S. J. Park, J. I. Jeong, S. H. Kim, J. Han, J. W. Kyung, S.-H. Baik, Y. Choi, B. Y. Choi, J. S. Park, G. Bahn, J. H. Shin, D. S. Jo, J.-Y. Lee, C.-G. Jang, T. V. Arumugam, J. Kim, J.-W. Han, J.-Y. Koh, D.-Y. Cho, D.-G. Jo. Inhibition of Drp1 ameliorates synaptic depression, Aβ deposition, and cognitive impairment in an Alzheimer's disease model. *J. Neurosci.* **37**, 5099–5110 (2017).

31. L. S. Griffith, B. Schmitz, *O*-linked *N*-acetylglucosamine is upregulated in Alzheimer brains. *Biochem. Biophys. Res. Commun.* **213**, 424–431 (1995).

32. S. Förster, A. S. Welleford, J. C. Triplett, R. Sultana, B. Schmitz, D. A. Butterfield, Increased *O*-GlcNAc levels correlate with decreased *O*-GlcNAcase levels in Alzheimer disease brain. *Biochim. Biophys. Acta* **1842**, 1333–1339 (2014).

33. X. Li, W. Gong, H. Wang, T. Li, K. S. Attri, R. E. Lewis, A. C. Kalil, F. Bhinderwala, R. Powers, G. Yin, L. E. Herring, J. M. Asara, Y. L. Lei, X. Yang, D. A. Rodriguez, M. Yang, D. R. Green, P. K.

Singh, H. Wen, *O*-GlcNAc transferase suppresses inflammation and necroptosis by targeting receptor-interacting serine/threonine-protein kinase 3. *Immunity* **50**, 576–590.e6 (2019).

34. B. Zhang, M.-D. Li, R. Yin, Y. Liu, Y. Yang, K. A. Mitchell-Richards, J. H. Nam, R. Li, L. Wang, Y. Iwakiri, D. Chung, M. E. Robert, B. E. Ehrlich, A. M. Bennett, J. Yu, M. H. Nathanson, X. Yang, *O*-GlcNAc transferase suppresses necroptosis and liver fibrosis. *JCI Insight* **4**, 127709 (2019).

35. C. Kim, D. W. Nam, S. Y. Park, H. S. Hong, J. H. Boo, E. S. Jung, Y. Kim, J. U. Baek, K. S. Kim, J. W. Cho, I. Mook-Jung, *O*-linked β-*N*-acetylglucosaminidase inhibitor attenuates β-amyloid plaque and rescues memory impairment. *Neurobiol. Aging* **34**, 275–285 (2013).

36. K. T. Jacobsen, K. Iverfeldt, *O*-GlcNAcylation increases non-amyloidogenic processing of the amyloid-β precursor protein (APP). *Biochem. Biophys. Res. Commun.* **404**, 882–886 (2011).

37. S. Jimenez, D. Baglietto-Vargas, C. Caballero, I. Moreno-Gonzalez, M. Torres, R. Sanchez-Varo, D. Ruano, M. Vizuete, A. Gutierrez, J. Vitorica, Inflammatory response in the hippocampus of PS1M146L/APP751SL mouse model of Alzheimer's disease: Age-dependent switch in the microglial phenotype from alternative to classic. *J. Neurosci.* **28**, 11650–11661 (2008).

38. K. Kawahara, M. Suenobu, A. Yoshida, K. Koga, A. Hyodo, H. Ohtsuka, A. Kuniyasu, N. Tamamaki, Y. Sugimoto, H. Nakayama, Intracerebral microinjection of interleukin-4/interleukin-13 reduces β-amyloid accumulation in the ipsilateral side and improves cognitive deficits in young amyloid precursor protein 23 mice. *Neuroscience* **207**, 243–260 (2012).

39. R.-Y. Pan, J. Ma, X.-X. Kong, X.-F. Wang, S.-S. Li, X.-L. Qi, Y.-H. Yan, J. Cheng, Q. Liu, W. Jin, C.-H. Tan, Z. Yuan, Sodium rutin ameliorates Alzheimer's disease–like pathology by enhancing microglial amyloid-β clearance. *Sci. Adv.* **5**, eaau6328 (2019).

40. I.-H. Ryu, K.-Y. Lee, S.-I. Do, Aβ-affected pathogenic induction of *S*-nitrosylation of OGT and identification of Cys-NO linkage triplet. *Biochim. Biophys. Acta* **1864**, 609–621 (2016).

41. A. Tramutola, N. Sharma, E. Barone, C. Lanzillotta, A. Castellani, F. Lavarone, F. Vincenzoni, M. Castagnola, D. A. Butterfield, S. Gaetani, T. Cassano, M. Perluigi, F. Di Domenico. Proteomic

identification of altered protein *O*-GlcNAcylation in a triple transgenic mouse model of Alzheimer's disease. *Biochim. Biophys. Acta Mol. Basis Dis.* **1864**, 3309–3321 (2018).

42. P. Sandhu, J. Lee, J. Ballard, B. Walker, J. Ellis, J. Marcus, D. Toolan, D. Dreyer, T. McAvoy, J. Duffy, M. Michener, C. Valiathan, N. Trainor, M. Savage, E. McEachern, D. Vocadlo, S. M. Smith, A. Struyk, Pharmacokinetics and pharmacodynamics to support clinical studies of MK-8719: An *O*-GlcNAcase inhibitor for progressive supranuclear palsy. *Alzheimers Dement.* **12**, P1028 (2016).

43. J. M. Ryan, A. Quattropani, K. Abd-Elaziz, I. den Daas, M. Schneider, S. Ousson, M. Neny, A. Sand, J. Hantson, B. Permanne, C. Wiessner, D. Beher. O1-12-05: Phase 1 study in healthy volunteers of the *O*-GlcNAcase inhibitor ASN120290 as a novel therapy for progressive supranuclear palsy and related tauopathies. *Alzheimers Dement.* **14**, P251 (2018).

44. B. T. Hyman, J. Q. Trojanowski, Consensus recommendations for the post-mortem diagnosis of Alzheimer disease from the National Institute on Aging and the Reagan Institute Working Group on diagnostic criteria for the neuropathological assessment of Alzheimer disease. *J. Neuropathol. Exp. Neurol.* **56**, 1095–1097 (1997).

45. G. Bahn, J.-S. Park, U. J. Yun, Y. J. Lee, Y. Choi, J. S. Park, S. H. Baek, B. Y. Choi, Y. S. Cho, H. K. Kim, J. Han, J. H. Sul, S.-H. Baik, J. Lim, N. Wakabayashi, S. H. Bae, J.-W. Han, T. V. Arumugam, M. P. Mattson, D.-G. Jo, NRF2/ARE pathway negatively regulates BACE1 expression and ameliorates cognitive deficits in mouse Alzheimer's models. *Proc. Natl. Acad. Sci. U.S.A.* **116**, 12516–12523 (2019).

46. A.-R. Gwon, J.-S. Park, T. V. Arumugam, Y.-K. Kwon, S. L. Chan, S.-H. Kim, S.-H. Baik, S. Yang, Y.-K. Yun, Y. Choi, S. Kim, S.-C. Tang, D.-H. Hyun, A. Cheng, C. E. Dann III, M. Bernier, J. Lee, W. R. Markesbery, M. P. Mattson, D.-G. Jo, Oxidative lipid modification of nicastrin enhances amyloidogenic γ-secretase activity in Alzheimer's disease. *Aging Cell* **11**, 559–568 (2012).

47. S.-H. Baik, M. Fane, J. H. Park, Y.-L. Cheng, D. Y.-W. Fann, U. J. Yun, Y. Choi, J.-S. Park, B. H. Chai, J. S. Park, S. H. Back, J. I. Jeong, Y. J. Jang, G. Bahn, J.-Y. Lee, Y.-I. Li, C. G. Sobey, T. Uchida, J. H. Park, H. T. Kim, S.-C. Tang, T. V. Arumugam, D.-G. Jo, Pin1 promotes neuronal death in stroke by stabilizing Notch intracellular domain. *Ann. Neurol.* **77**, 504–516 (2015).

48. H. Y. Kim, D. K. Lee, B.-R. Chung, H. V. Kim, Y. Kim, Intracerebroventricular injection of amyloid-β peptides in normal mice to acutely induce Alzheimer-like cognitive deficits. *J. Vis. Exp.* **109**, e53308 (2016).

49. J. Park, M. Madan, S. Chigurupati, S. H. Baek, Y. Cho, M. R. Mughal, A. Yu, S. L. Chan, J. V. Pattisapu, M. P. Mattson, D.-G. Jo, Neuronal Aquaporin 1 inhibits amyloidogenesis by suppressing the interaction between beta-secretase and amyloid precursor protein. *J. Gerontol. A Biol. Sci. Med. Sci.*, glaa068 (2020).

50. L. Zhang, F. Ren, J. Li, X. Ma, P. Wang. A modified coupled enzyme method for *O*-linked GlcNAc transferase activity assay. *Biol. Proced. Online* **11**, 170–183 (2009).

51. Y. He, X. Ma, D. Li, J. Hao Thiamet G mediates neuroprotection in experimental stroke by modulating microglia/macrophage polarization and inhibiting NF-κB p65 signaling. *J. Cereb. Blood Flow Metab.* **37**, 2938–2951 (2017).

52. C. Rossi, M. Cusimano, M. Zambito, A. Finardi, A. Captondo, J. M. Garcia-Manteiga, G. Comi, R. Furlan, G. Martino, L. Muzio. Interleukin 4 modulates microglia homeostasis and attenuates the early slowly progressive phase of amyotrophic lateral sclerosis. *Cell Death Dis.* **9**, 250 (2018).